Dephasing and pseudocoherent quantum dynamics in super-Ohmic environments

Ph. Nacke [1], F. Otterpohl [2], M. Thorwart [2,3] and P. Nalbach [1]

[1] *Fachbereich Wirtschaft & Informationstechnik, Westfälische Hochschule, Münsterstrasse 265, 46397 Bocholt, Germany*

[2] *I. Institut für Theoretische Physik, Universität Hamburg, Notkestraße 9, 22607 Hamburg, Germany*

[3] *The Hamburg Centre for Ultrafast Imaging, Luruper Chaussee 149, 22761 Hamburg, Germany*

(Received 31 March 2023; accepted 20 June 2023; published 28 June 2023)

Dephasing in quantum systems is typically the result of their interaction with environmental degrees of freedom. We investigate within a spin-boson model the influence of a super-Ohmic environment on the dynamics of a quantum two-state system. A super-Ohmic environment thereby models typical bulk phonons which are a common disturbance for solid state quantum systems as, for example, nitrogen-vacancy centers. By applying the numerically exact quasiadiabatic path-integral approach we show that for strong system-bath coupling, pseudocoherent dynamics emerges, i.e., oscillatory dynamics at short times due to slaving of the quantum system to the bath dynamics. We extend the phase diagram known for sub-Ohmic and Ohmic environments into the super-Ohmic regime and observe a pronounced nonmonotonous behavior. Super-Ohmic purely dephasing fluctuations strongly suppress the amplitude of coherent dynamics at very short times with no subsequent further decay at later times. Nevertheless, they render the dynamics overdamped. The corresponding phase separation line shows also a nonmonotonous behavior, very similar to the pseudocoherent dynamics.

DOI: 10.1103/PhysRevA.107.062218

I. INTRODUCTION AND MOTIVATION

Dissipation, i.e., dephasing and relaxation, in a quantum system is a result of its coupling to environmental fluctuations. At strong coupling the dissipative environment may also lead to fully incoherent dynamics or even complete suppression of the coherent quantum dynamics (localization). Theoretical studies typically reduce the relevant quantum system to a paradigmatic two-state quantum system with the model Hamiltonian $H_0 = \Delta\sigma_x/2$ with tunnel element Δ and Pauli matrices σ_j (with $j = x, y, z$), interacting with harmonic degrees of freedom [1,2] which act as the dissipative environment. The central characteristic of the environmental fluctuations is their spectral distribution which is typically modeled as a continuous function of frequency ω, increasing $\propto\alpha\omega^s$ with spectral exponent s and coupling strength α. It is denoted as sub-Ohmic, Ohmic, and super-Ohmic for $0 < s < 1$, $s = 1$, and $s > 1$, respectively.

Usually, one addresses *relaxational* fluctuations which cause transitions in the two-state system (via a coupling to σ_z) and thus relaxation. The corresponding model is termed the spin-boson model [1,2] and shows in the Ohmic case with increasing α at $\alpha = \alpha_o(s = 1) = \frac{1}{2}$ for the expectation value $P_z(t) = \langle\frac{1}{2}\sigma_z(t)\rangle$ [and likewise for the correlation function $\langle\sigma_z(t)\sigma_z(0)\rangle$] a dynamic transition from coherent oscillatory behavior to incoherent dynamics. Incoherent dynamics [1,2] occurs when the oscillatory frequency is renormalized to zero at a finite system-bath coupling α. The dynamics might be effectively overdamped (when the damping rate exceeds the oscillatory frequency) already at lower couplings. When increasing the coupling strength further to $\alpha = \alpha_c(s = 1) = 1$, the Ohmic spin-boson model exhibits at zero temperature a quantum phase transition into a localized phase with a degenerate ground state, i.e., the eigenstates to σ_z. A sub-Ohmic environment shows similar behavior [3–9] depending on the spectral exponent s, but a super-Ohmic environment exhibits only damped oscillatory behavior [1,2].

Super-Ohmic reservoirs receive fairly little consideration in theoretical studies since the dynamics turns neither localized nor incoherent even at strongest coupling except at high temperatures [10]. Super-Ohmic reservoirs are, however, fairly common and are, for example, the cause of damping for all dipolar defects in nonconducting solids, i.e., when phonons are the main noise source. Prominent examples are tunneling two-level systems in amorphous systems, glasses [11,12] and crystals [13], but also nitrogen-vacancy (NV) and silicon-vacancy (SiV) centers in diamonds [14–16]. In these cases the spectral exponent is $s = 3$. Super-Ohmic reservoirs are also relevant noise sources for charge double quantum dots [17] and for energy transfer in the Fenna-Matthews-Olson (FMO) exciton transfer complex [18]. In the latter case a spectral exponent $s = 5$ was proposed.

For the sub-Ohmic and the Ohmic bath, recently a particular dynamic behavior at short times at strongest coupling was revealed (termed pseudocoherent) initially exhibiting in $P_z(t)$ an oscillatory behavior with at least a single minimum [19]. This oscillatory polarization dynamics results from the two-state system being slaved to the bath which itself shows coherent dynamics on a timescale ω_c^{-1} due to a finite upper cutoff frequency ω_c of the environmental fluctuations. On any other timescale the quantum system shows no oscillatory (coherent) dynamics at these coupling strengths. In the scaling limit $\omega_c \to \infty$ the pseudocoherent oscillatory behavior shifts to earlier times and finally vanishes. Although relaxational super-Ohmic fluctuations [1,2] cause neither localization nor overdamping, we show in this paper numerically (as our first result) that for strong system-bath coupling, pseudocoherent dynamics, i.e., oscillatory dynamics at short times due to

slaving the quantum system to bath dynamics, is present. We determine the minimal coupling strength $\alpha_B(s)$, at which pseudocoherent dynamics sets in, as a function of the spectral exponent s of the environmental fluctuations. This extends the phase diagram of the pseudocoherent dynamics into the super-Ohmic regime. Surprisingly, $\alpha_B(s)$ as a function of s is nonmonotonic and shows a maximum at $s \simeq 2$.

In addition, we consider *purely dephasing* super-Ohmic fluctuations, i.e., the system-bath coupling operator is $\propto\sigma_x$. The corresponding model is termed an independent-boson model [20] and we find that purely dephasing super-Ohmic fluctuations do not cause an exponential decay of coherence. Instead, after an initial Gaussian decay [21] for a timescale ω_c^{-1}, no further dephasing occurs at later times. The dynamics remains coherent but this strongly non-Markovian short-time behavior severely diminishes its amplitude. For strong system-bath coupling the dynamics is effectively overdamped and an effective transition coupling strength can be determined. Mapping out this transition as a function of s, it shows surprisingly a very similar nonmonotonic behavior as the pseudocoherent phase. Finally, we show that realistic quantum systems, which are exposed to both types of fluctuations, exhibit an initial fast dephasing due to the purely dephasing fluctuations. It subsequently saturates, and is followed by an additional exponentially decay due to the relaxational fluctuations.

In the following, we present the studied model and shortly describe the used numerical methods in Sec. II. In Secs. III–V, results for the pseudocoherent behavior, the Gaussian decay behavior, and the mixed case are discussed before we conclude.

II. MODEL AND NUMERICAL METHOD

The Hamiltonian ($\hbar = 1$)

$$H = \frac{\Delta}{2}\sigma_x + (u_x\sigma_x + u_z\sigma_z)\sum_k \lambda_k \hat{q}_k + H_B \qquad (1)$$

describes a quantum two-state system with tunneling element Δ which is coupled by λ_k to the displacements $\hat{q}_k$ of the harmonic environmental fluctuations $H_B = \frac{1}{2}\sum_k(\hat{p}_k^2 + \omega_k^2\hat{q}_k^2)$ with frequency ω_k. Herein, the case $u_x = 0$ and $u_z = 1$ reflects coupling to relaxational fluctuations (spin-boson model) whereas the case of purely dephasing fluctuations is given by $u_z = 0$ and $u_x = 1$ (independent-boson model).

The spectral function of the fluctuations is

$$G(\omega) = \sum_k \frac{\lambda_k^2}{2\omega_k}\delta(\omega - \omega_k) = 2\alpha\omega_s^{1-s}\omega^s e^{-\omega/\omega_c}, \qquad (2)$$

with spectral exponent s and a maximal environmental frequency (cutoff frequency) ω_c. The frequency ω_s serves to keep the coupling strength α dimensionless and we fix $\omega_s = \omega_c$.

We calculate the time-dependent polarization $P_z(t) = \langle\frac{1}{2}\sigma_z\rangle_t$, using a factorizing initial preparation of the system with $P_z(0) = \frac{1}{2}$ and the thermal distribution of the bath at zero temperature. To determine $P_z(t)$ for relaxational fluctuations ($u_x = 0$ and $u_z = 1$) we use the numerically exact real-time quasiadiabatic propagator path integral (QUAPI) [22–25]. Once the bath oscillators have been integrated out, an effective dynamics of the system arises which is nonlocal in time. To treat the highly entangled system-bath dynamics, we make use of the time-evolving matrix product operator (TEMPO) technique in terms of a numerically highly efficient tensor network [26]. Purely dephasing fluctuations are analytically tractable within the independent boson model [20] which was already successfully employed for the Ohmic case [27–29] and the sub-Ohmic case [9]. Accordingly, $P_z(t)$ is determined exactly in this case.

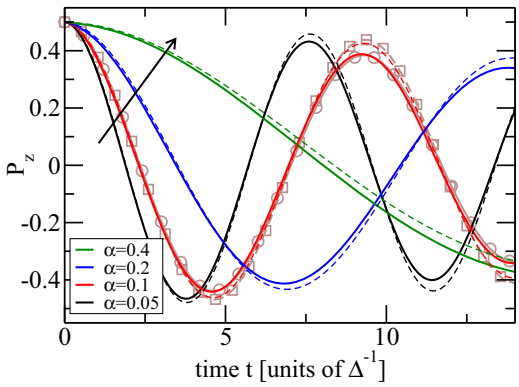

FIG. 1. Polarization $P_z(t)$ vs time for various values of the coupling strength α and a spectral exponent $s = 2$ for $\omega_c = 10\Delta$ (solid lines) and $\omega_c = 20\Delta$ (dashed lines) at $T = 0$. The brown lines lines represent weak-coupling approximations [1] to the $\alpha = 0.1$ results. Since they agree very well with the numerical results, the brown lines are hardly visible. Thus, we added symbols in brown (solid with circle symbols and dashed with square symbols) which highlights that brown and red lines are (almost) identical. The arrows indicate increasing coupling strength.

III. NUMERICAL RESULTS FOR THE SUPER-OHMIC SPIN-BOSON MODEL

In the following we study the influence of a relaxational super-Ohmic bath ($u_x = 0$ and $u_z = 1$) at zero temperature on the dynamics of a quantum two-state system. Figure 1 shows the polarization $P_z(t)$ versus time for various values of the coupling strength α and a spectral exponent $s = 2$ for $\omega_c = 10\Delta$ (solid lines) and $\omega_c = 20\Delta$ (dashed lines). The polarization exhibits damped oscillations following the well-known weak-coupling expression [1] $P_z(t) = \frac{1}{2}\cos(\Delta_{\rm eff}t)\exp(-\gamma_{\rm eff}t)$. The oscillation frequency is renormalized due to the coupling to environmental fluctuations, i.e., with increasing coupling strength α the frequency is decreased [1], following $\Delta_{\rm eff} = \Delta\exp(-\widetilde{\alpha})$ with $\widetilde{\alpha} = 4\alpha\Gamma(s-1)$ with the gamma function $\Gamma(x)$. Note that the frequency renormalization is independent of ω_c. The observed weak damping is fully described by the one-phonon rate [1] $\gamma_{\rm eff} = (2\pi)\alpha\Delta_{\rm eff}^2/\omega_c$ (for $s = 2$ and $T = 0$) which shows a dependence on ω_c (compare solid with dashed lines in Fig. 1). The brown solid and dashed lines (with circle and square symbols, respectively) in Fig. 1 are the analytical expectations for the numerically determined red lines for $\alpha = 0.1$ and we observe good agreement between both. Note that we added circle (square) symbols to the solid (dashed) brown line to point out the brown lines which are mainly covered by the red ones.

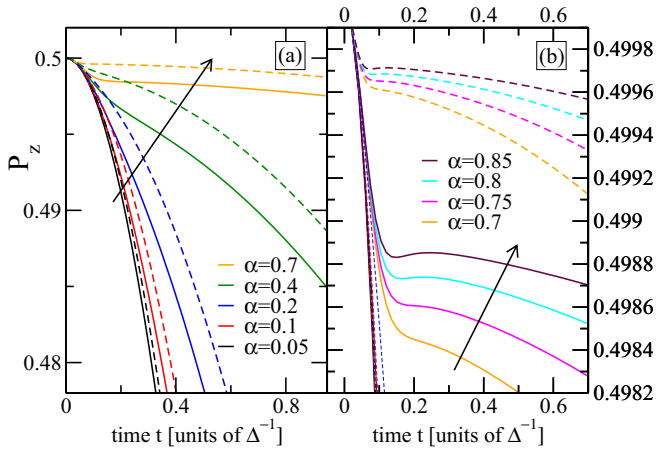

FIG. 2. Polarization $P_z(t)$ vs time for various values of the coupling strength α and a spectral exponent $s = 2$ for $\omega_c = 10\Delta$ (solid lines) and $\omega_c = 20\Delta$ (dashed lines) at $T = 0$. The graphs show different time and amplitude regimes. The arrows indicate increasing coupling strength.

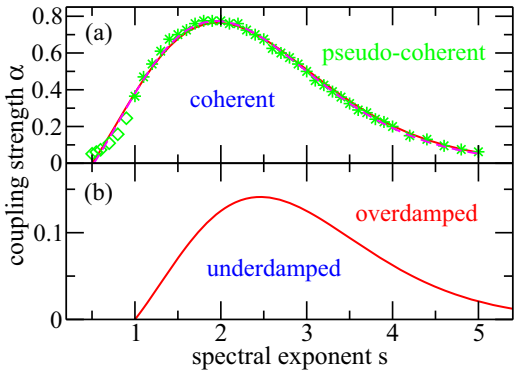

FIG. 3. (a) The green stars are the numerically determined transition coupling strength $\alpha_B(s)$ for the crossover to pseudocoherent dynamics in the super-Ohmic relaxational bath. The green diamonds are the corresponding data for $s < 1$ taken from Ref. [19]. The red line is a fit with $A/[8\Gamma(s-\frac{1}{2})]$ resulting in $A = 5.42$ and the magenta line is a fit with $A/[8\Gamma(B\cdot s - C)]$ resulting in $A = 5.487$, $B = 1.026$, and $C = 0.5342$. (b) The red solid line reflects the transition $\alpha_o(s)$ to overdamped behavior in the super-Ohmic purely dephasing bath. Parameters in both panels are $\omega_c = 10\Delta$ and $T = 0$.

Figure 2 shows the polarization $P_z(t)$ versus time for the same parameters as above and also larger coupling strengths. Focusing on small times we observe at times roughly ω_c^{-1} the emergence of a minimum in the dynamics [focused on in Fig. 2(b) with solid lines for $\omega_c = 10\Delta$ and dashed lines for $\omega_c = 20\Delta$]. This minimum is similar to the pseudocoherent behavior observed for $s \leqslant 1$ in Ref. [19]. With increasing coupling, the pseudocoherent minimum shifts towards earlier times. Since the dynamics is not localized for $s > 1$, it is hard to resolve the shallow minimum and thus $\alpha_B(s)$. The accuracy depends on the maximally simulated time $t_{\max}$. For $1.0 \leqslant s \leqslant 1.3$ we used $t_{\max} = 3\Delta^{-1}$ and for larger s we used $t_{\max} = \Delta^{-1}$. For $\omega_c = 20\Delta$ we observe qualitatively the same behavior as for $\omega_c = 10\Delta$ (compare Fig. 2). The absolute value of $P_z(t)$ at the pseudocoherent minimum increases with ω_c. Surprisingly, the transition coupling strength α_B does not change with ω_c.

In Fig. 3(a) we show the phase diagram of the super-Ohmic pseudocoherent behavior. The green stars are the numerically determined transition coupling strengths $\alpha_B(s)$ for the crossover to pseudocoherent dynamics, i.e., where the minimum in the dynamics emerges. The green diamonds are the corresponding data for $s < 1$ taken from Ref. [19]. The phase separation line shows a strong nonmonotonous behavior with a peak for $s \simeq 2$. It smoothly connects to the results of Ref. [19]. Note the difference of a factor $\frac{1}{2}$ in the system-bath coupling in Hamiltonian (1) which results in a factor of 4 difference between our coupling strength and the one given in Ref. [19]. The magenta line in Fig. 3(a) is a fit with $A/[8\Gamma(B\cdot s - C)]$ resulting in optimal values $A = 5.487$, $B = 1.026$, and $C = 0.5342$. The red line (which falls on top of the magenta line) is a fit with the simplified function $A/[8\Gamma(s-\frac{1}{2})]$ resulting in $A = 5.42$. Both fits reasonably describe the peak and the data for $s \gtrsim 1$, i.e., for the super-Ohmic regime. For $s \leqslant 1$ (sub-Ohmic and Ohmic regime) the fit does not describe the data sufficiently well.

IV. ANALYTICAL RESULTS FOR THE SUPER-OHMIC INDEPENDENT-BOSON MODEL

The case of a purely dephasing bath with diagonal coupling ($u_x = 1$ and $u_z = 0$) can be studied analytically. Employing the transformation $T_P = e^{i\psi\sigma_x}$ with $\psi = \sum_k \frac{\lambda_k}{\omega_k^2}\hat{p}_k$ results in $H_P = T_P^\dagger H T_P = \Delta\sigma_{x,P}/2 + H_B$ with $\sigma_{x,P} = T_P^\dagger\sigma_x T_P = \sigma_x$. Thus, the propagator $U_P = e^{-iH_P t}$ is determined by a direct product of system and bath operators. At the same time, $\sigma_{z,P} = T_P^\dagger\sigma_z T_P = \sigma_z\cos\psi - \sigma_y\sin\psi$. When measuring the polarization, we initially displace the system fully, i.e., $P_z(0) = \frac{1}{2}$. Thus, $\langle\sigma_x\rangle = 0$ and if the bath is allowed to equilibrate to this situation before the experiment starts, we can assume a factorized initial condition $\rho_{0,P_z} = \rho(t=0) = \frac{1}{2}(\mathbb{1}+\sigma_z)\otimes\rho_{B,\mathrm{eq}}$ with $\rho_{B,\mathrm{eq}} = Z_B^{-1}e^{-\beta H_B}$ and $Z_B = \mathrm{Tr}\{e^{-\beta H_B}\}$ and $\beta = (k_B T)^{-1}$ for temperature T. A tedious calculation then results in the polarization

$$P_z(t) = \frac{1}{2}\cos(\Delta t)e^{-\Gamma_T(t)}, \tag{3}$$

with the decay function

$$\Gamma_T(t) = 4\int_0^\infty d\omega\frac{G(\omega)}{\omega^2}[1-\cos\omega t]\coth(\beta\omega/2). \tag{4}$$

Note that no frequency renormalization occurs here and that the decay function is dominated by high-frequency modes, in contrast to pure dephasing decay for sub-Ohmic and Ohmic baths. At zero temperature we find for super-Ohmic fluctuations $s > 1$,

$$\Gamma_0(t,s) = \widetilde{\alpha}\left\{1 - \frac{\cos[(s-1)\arctan(\omega_c t)]}{[1+(\omega_c t)^2]^{(s-1)/2}}\right\}, \tag{5}$$

with the effective coupling $\widetilde{\alpha} = 8\alpha\Gamma(s-1)$ and the gamma function $\Gamma(x)$.

Initially, at times $\omega_c t \ll 1$ [and $(s-1) \lesssim 10$], we observe a spectral diffusion type of Gaussian decay: $\Gamma_0(t,s) \simeq \widetilde{\alpha}\frac{1}{2}(s^2-s+2)(\omega_c t)^2$. At later times, $\omega_c t \gtrsim 1$, the decay

function becomes constant, i.e., $\Gamma_0(t,s) \simeq \widetilde{\alpha}$, and no further dephasing takes place. Thus, as long as $\widetilde{\alpha} \ll 1$, dephasing is negligible. If $\widetilde{\alpha} \gtrsim 1$, however, even though $\Gamma_0(t,s)$ becomes constant, dephasing suppresses the response to negligible values. Thus, although strictly speaking the dynamics is oscillatory, the amplitude is vanishingly small and the dynamics is effectively overdamped, i.e., not a single sizable oscillation takes place. Defining $\widetilde{\alpha}_o \equiv 1$ as the transition point, we find

$$\alpha_o(s) = \frac{1}{8\Gamma(s-1)}, \tag{6}$$

which we plot in Fig. 3(b) by the solid red line. We observe a strongly nonmonotonous behavior with a peak at roughly $s \simeq 2.5$. Surprisingly, this peak strongly resembles the observed behavior for the transition to pseudocoherent dynamics although the peak is slightly shifted and the maximal value is considerably smaller. Testing this observation we employed the fit function $A/[8\Gamma(B \cdot s - C)]$ with fit parameters A, B, and C above to fit $\alpha_B(s)$ as a function of s resulting in the magenta line in Fig. 3(a). Fixing $B = 1$ and $C = 0.5$ does not deteriorate the fit and then we obtain $A = 5.42$ [red line in Fig. 3(a)]. Note that $\alpha_o(s)$ also does not depend on ω_c, similar to our observation for $\alpha_B(s)$.

V. EXPERIMENTAL RELEVANCE OF PURELY DEPHASING FLUCTUATIONS

The influence of relaxational super-Ohmic fluctuations on the dynamics of a quantum system is readily observable in the population decay as well as in the form of decoherence. Dephasing due to super-Ohmic purely dephasing fluctuations is restricted to times much shorter than typical system times, i.e., Δ^{-1}, as for most solid state systems $\omega_c^{-1} \ll \Delta^{-1}$ holds. The amplitude of the polarization oscillations is diminished but on timescales Δ^{-1} no further decay occurs. When measuring an ensemble the overall experimental response is proportional to the number of systems in the ensemble. This quantity is typically not precisely accessible and thus the dephasing cannot be detected. Thus, often theoretical studies, focused on weak Markovian environments, completely neglect super-Ohmic purely dephasing. For qubit applications, however, survival of the coherence of single systems, for example, in NV centers, after initial preparation is key. Dephasing at any timescale shorter than a typical time needed to perform a gate operation on a qubit, which is typically much longer than Δ^{-1}, deteriorates qubit applications.

It remains to study whether a system under the influence of both relaxational and purely dephasing fluctuations, which seems experimentally the most likely situation, suffers the dephasing behavior of purely dephasing fluctuations as discussed above. The Hamiltonian in Eq. (1) with $u_x = \sin\phi \neq 0 \neq u_z = \cos\phi$ can be transformed to

$$H = \frac{\Delta}{2}\cos\phi\,\sigma_x + \frac{\Delta}{2}\sin\phi\,\sigma_z + \sigma_z \sum_k \lambda_k \hat{q}_k + H_B,$$

i.e., an asymmetric spin-boson model. Figure 4 plots the polarizations $P_z(t) = \langle \frac{1}{2}\sigma_z \rangle_t$ and $P_x(t) = \langle \frac{1}{2}\sigma_x \rangle_t$ in the transformed basis versus time for coupling strength $\alpha = 0.2$, a spectral exponent $s = 2$, $\omega_c = 10\Delta$, and $\Delta\cos\phi = 1 = \Delta\sin\phi$. In this transformed basis both $P_z(t)$ and $P_x(t)$ exhibit thermalization and decoherence features. $P_z(t)$ shows at short times [Fig. 4(a)], i.e., $t \lesssim 0.1\Delta^{-1} = \omega_c^{-1}$, a sharp Gaussian-type decay down to roughly $e^{-\widetilde{\alpha}}$. At later times [Fig. 4(b)], the oscillation amplitude decays further but with a much smaller rate which is comparable to the dephasing rate observed in the symmetric spin-boson model for similar parameters (see Fig. 1). Thus, indeed the dynamics in the asymmetric spin-boson model exhibits dephasing features of both the relaxational and the purely dephasing fluctuations independently observed above. Note that standard weak-coupling analytical expressions [1] for the asymmetric spin-boson model, i.e., $P_z(t) = (\Delta_{\rm eff}/E)^2\cos(Et)\exp(-\gamma_{\rm eff}t) + (\Delta/E)^2\exp(-2\gamma_{\rm eff}t) + (\Delta/E)[1-\exp(-2\gamma_{\rm eff}t)] + O(\gamma_{\rm eff}/E)$ with $E = \sqrt{\Delta_{\rm eff}^2 + \Delta^2}$, do not include the Gaussian-type decay at early times since their derivation is based on the assumption that relevant timescales are much longer than ω_c^{-1}.

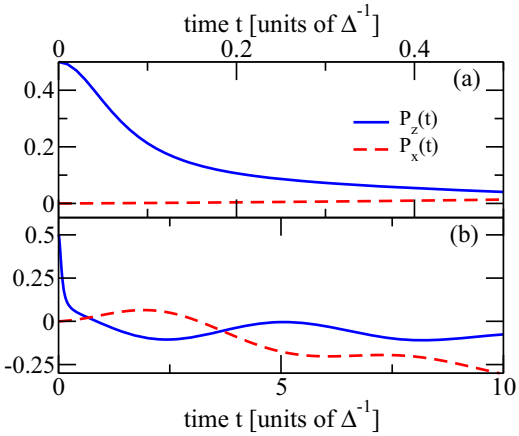

FIG. 4. Polarization $P_z(t)$ and $P_x(t)$ in the asymmetric super-Ohmic spin-boson model vs time for coupling strength $\alpha = 0.2$, a spectral exponent $s = 2$, and $\omega_c = 10\Delta$ at $T = 0$. (a) $P_z(t)$ and $P_x(t)$ are displayed at short times $t \leqslant 0.5\Delta^{-1}$. (b) $P_z(t)$ and $P_x(t)$ are displayed for times $t \leqslant 10\Delta^{-1}$.

VI. CONCLUSIONS

We have investigated the polarization dynamics of a quantum two-state system coupled to a super-Ohmic environment within a spin-boson model. Super-Ohmic environments are fairly common in solid state quantum systems as they model typical bulk phonons. Prominent quantum systems subject to super-Ohmic environments are NV centers [14–16]. For the treatment of relaxational environmental fluctuations and the study of the polarization dynamics we employ the numerical exact quasiadiabatic path integral approach combined with an efficient tensor network treatment. Purely dephasing fluctuations alone are treated analytically. The combination of both again requires numerical treatment.

Super-Ohmic environments cannot turn the dynamics localized or incoherent. On the timescale of the bare quantum system, however, the dynamics is severely slowed down since the oscillation frequency of the polarization is strongly decreased with increasing system-bath coupling. At strong coupling we observe pseudocoherent dynamics, i.e.,

oscillatory dynamics at short times due to slaving the quantum system to bath dynamics. We map the minimal coupling strength $\alpha_B(s)$, at which pseudocoherent dynamics occurs, as a function of the spectral exponent s of the environmental fluctuations and thus extend the phase diagram of the pseudocoherent dynamics [19] into the super-Ohmic regime. Surprisingly, $\alpha_B(s)$ as a function of s is nonmonotonic with a maximum at $s \simeq 2$. Purely dephasing super-Ohmic fluctuations cause an initial Gaussian decay for a timescale ω_c^{-1} and then no further dephasing. Nevertheless the coherence amplitude is severely diminished at strong coupling, rendering the dynamics effectively overdamped. The corresponding phase separation line of coupling versus spectral exponent exhibits also nonmonotonous behavior, very similar to the pseudocoherent phase.

Realistic quantum systems are typically exposed to both types of environmental fluctuations, i.e., purely dephasing and relaxational ones. We show that the polarization dynamics then exhibits a fast initial Gaussian decay followed by the much slower (for the same system-bath coupling) exponential decay due to the relaxational fluctuations. Hence, neglecting the non-Markovian Gaussian decay due to the purely dephasing fluctuations may not be justified when studying the coherence of a quantum system as is relevant for quantum devices. Even at weak system-bath coupling α the inflicted decay is proportional $\propto \exp(-\widetilde{\alpha})$ with $\widetilde{\alpha} = 8\alpha\Gamma(s-1)$ and the gamma function $\Gamma(x)$ and might well be relevant for the envisioned quantum device. Dynamical decoupling schemes are also not effective to counter super-Ohmic dephasing since it is dominantly a result of high-frequency environmental modes whereas dynamical decoupling counteracts mainly low-frequency noise.

ACKNOWLEDGMENTS

M.T. acknowledges support by the Cluster of Excellence CUI: Advanced Imaging of Matter of the Deutsche Forschungsgemeinschaft (DFG) – EXC 2056 – Project ID 390715994.

[1] U. Weiss, *Quantum Dissipative Systems*, 5th ed. (World Scientific, Singapore, 2021).
[2] A. J. Leggett, S. Chakravarty, A. T. Dorsey, M. P. A. Fisher, A. Garg, and W. Zwerger, Rev. Mod. Phys. **59**, 1 (1987).
[3] F. B. Anders, R. Bulla, and M. Vojta, Phys. Rev. Lett. **98**, 210402 (2007).
[4] A. Winter, H. Rieger, M. Vojta, and R. Bulla, Phys. Rev. Lett. **102**, 030601 (2009).
[5] A. Alvermann and H. Fehske, Phys. Rev. Lett. **102**, 150601 (2009).
[6] P. Nalbach and M. Thorwart, Phys. Rev. B **81**, 054308 (2010).
[7] C. Guo, A. Weichselbaum, J. von Delft, and M. Vojta, Phys. Rev. Lett. **108**, 160401 (2012).
[8] D. Kast and J. Ankerhold, Phys. Rev. Lett. **110**, 010402 (2013).
[9] P. Nalbach and M. Thorwart, Phys. Rev. B **87**, 014116 (2013).
[10] A. Würger, Phys. Rev. Lett. **78**, 1759 (1997).
[11] J. Jäckle, Z. Phys. **257**, 212 (1972).
[12] P. Nalbach, D. D. Osheroff, and S. Ludwig, J. Low Temp. Phys. **137**, 395 (2004).
[13] P. Nalbach, O. Terzidis, K. A. Topp, and A. Würger, J. Phys.: Condens. Matter **13**, 1467 (2001).
[14] A. Alkauskas, B. B. Buckley, D. D. Awschalom, and C. G. Van de Walle, New J. Phys. **16**, 073026 (2014).
[15] K. D. Jahnke, A. Sipahigil, J. M. Binder, M. W. Doherty, M. Metsch, L. J. Rogers, N. B. Manson, M. D. Lukin, and F. Jelezko, New J. Phys. **17**, 043011 (2015).
[16] A. Norambuena, S. A. Reyes, J. Mejía-Lopéz, A. Gali, and J. R. Maze, Phys. Rev. B **94**, 134305 (2016).
[17] P. Nalbach, J. Knörzer, and S. Ludwig, Phys. Rev. B **87**, 165425 (2013).
[18] T. Renger and R. A. Marcus, J. Chem. Phys. **116**, 9997 (2002).
[19] F. Otterpohl, P. Nalbach, and M. Thorwart, Phys. Rev. Lett. **129**, 120406 (2022).
[20] G. D. Mahan, *Many-Particle Physics* (Kluwer Academic/Plenum, New York, 1981).
[21] D. Braun, F. Haake, and W. T. Strunz, Phys. Rev. Lett. **86**, 2913 (2001).
[22] N. Makri, J. Math. Phys. **36**, 2430 (1995).
[23] N. Makri and D. E. Makarov, J. Chem. Phys. **102**, 4600 (1995).
[24] N. Makri and D. E. Makarov, J. Chem. Phys. **102**, 4611 (1995).
[25] T. Palm and P. Nalbach, J. Chem. Phys. **149**, 214103 (2018).
[26] A. Strathearn, P. Kirton, D. Kilda, J. Keeling, and B. W. Lovett, Nat. Commun. **9**, 3322 (2018).
[27] G. M. Palma, K.-A. Suominen, and A. K. Ekert, Proc. R. Soc. London, Ser. A **452**, 567 (1996).
[28] J. H. Reina, L. Quiroga, and N. F. Johnson, Phys. Rev. A **65**, 032326 (2002).
[29] H.-S. Goan, C.-C. Jian, and P.-W. Chen, Phys. Rev. A **82**, 012111 (2010).